

Local-mode approximations in the Frenkel-Kontorova or sine-Gordon chain

D. Perchak and J. H. Weiner

Department of Physics and Division of Engineering, Brown University, Providence, Rhode Island 02912

(Received 6 May 1980)

Local-mode-approximation methods previously developed for the study of dislocation or kink dynamics in the modified Frenkel-Kontorova model or sine-Gordon chain in the absence of viscosity are here extended to the case in which viscous forces are present. It is found that the effect of viscosity is to increase the accuracy of the local-mode approximation at $T = 0$ K. Computer simulation results are presented for the average dislocation velocity as a function of applied stress for $T > 0$ K as well as for $T = 0$ K. The local-mode approximation leads to a pendulum analogy, involving inelastic collisions between successive pendulums, which shows a close relation between the Brownian motion of kinks in the sine-Gordon chain and the motion of a single Brownian particle in a periodic potential.

I. INTRODUCTION

The model of a linear chain of atoms interconnected by linear springs and subjected to a sinusoidal substrate potential is now generally referred to as a sine-Gordon chain. It is currently widely studied both because of its intrinsic mathematical interest^{1,2} and because of the large number of physical situations for which the model represents the simplest formulation which includes the essence of the process. Areas of application include one-dimensional ferromagnets with planar anisotropy,^{3,4} pinned charge-density waves,⁵ and interfacial layers separating phases in a two-phase⁶ system. An extensive review is given by Barone *et al.*⁷

An early—perhaps the earliest—use of this model was made by Frenkel and Kontorova⁸ for the study of the dynamics of dislocations in crystals, and in this field it is known as the Frenkel-Kontorova model.⁹ It has been used extensively in subsequent studies of dislocations; a review of some of this work may be found in the treatise by Nabarro.¹⁰

A modification of the Frenkel-Kontorova model was introduced by Kratochvil and Indenbom¹¹ and by Weiner and Sanders¹² (hereafter referred to as I) in which the sinusoidal substrate potential was replaced by one defined by a piecewise quadratic periodic function.¹³ The modified Frenkel-Kontorova model is more tractable analytically than the original version since its defining equations are piecewise linear. At the same time, the use of the piecewise quadratic substrate potential permits the study of a broader class of potential shapes ranging from cusped¹⁴ or very sharp potential peaks to ones which are very broad. The dynamics of dislocations in the modified Frenkel-Kontorova model has been studied extensively,¹⁵⁻¹⁸ both analytically and by computer simulation tech-

niques. Most of the work has been at $T = 0$ K, but some attempts have been made to incorporate thermal effects.^{19,20} Some studies have also used two-dimensional piecewise linear models for dislocations.^{21,22}

The piecewise linearity of the modified Frenkel-Kontorova model leads to linear difference equations with simple analytical solutions for the static configurations of the atoms in the presence of a dislocation or kink (I) and for the critical driving stress required to move a dislocation quasistatically from one equilibrium configuration to an adjacent one. For the study of steadily moving dislocations, the piecewise linearity of the model has also permitted the use of integral transform methods. Two phenomena of interest treated in this way are (a) the ability of a dislocation in the discrete model to move at particular velocities (at $T = 0$ K) with no radiative losses (i.e., no "phonon wake") and no driving stress required,²³ and (b) the breakdown of regular motion of the dislocation when its velocity approaches the sound speed in the chain.^{24,25} The latter phenomenon has also been studied by computer simulation in a two-dimensional model.²¹

The nature of the normal modes of vibration of the modified Frenkel-Kontorova model has been studied in I and it has been found that, for a wide range of parameter values, localized modes exist whose magnitudes are large only in the vicinity of the dislocation and that such modes exist when the dislocation is in either the stable or unstable equilibrium configuration. These localized modes were used by Weiner¹⁵ (hereafter referred to as II) as the basis of an approximate analytical method for the study of dislocation dynamics.

Much of the current research on the sine-Gordon chain deals with its Brownian motion. For this purpose, viscous and random thermal forces are added and the defining equation of the model takes

the form of a Langevin equation. One of the principal purposes of the present work is to test the utility of the local-mode approximation used in the absence of viscosity in II when viscous forces are present. A second purpose is to study, by computer simulation and within the Langevin equation framework, the effect of thermal motion upon dislocation velocities.

The plan of this paper is as follows: The defining equations of the model are summarized in Sec. II and the local-mode approximation is reviewed in Sec. III. It is used there to compute, as a function of the viscosity, the minimum stress required to maintain the steady motion at $T=0$ K of the dislocation along the chain once it has been set into motion. This stress, termed in II the dynamic Peierls stress σ_{PD} , is less than the Peierls stress σ_P required to move the dislocation quasistatically from one equilibrium position to an adjacent one. Computer simulation techniques for the model both for $T=0$ K and $T>0$ K are presented in Sec. IV and results of calculations using these techniques are given in Sec. V for $T=0$ and in Sec. VI for $T>0$ K. Conclusions are summarized in Sec. VII.

II. MODEL DESCRIPTION

As in the sine-Gordon chain, the model consists of atoms which interact via springs of equilibrium spacing b and spring constant k_1 and in addition are subject to a periodic substrate potential of period b . The particles are also driven by an external field, here represented²⁶ as an applied stress $\bar{\sigma}$. The surrounding medium is regarded as a heat bath and provides the source for thermal effects. This heat-bath interaction is described by means of a Langevin equation in which the influence of the heat bath on the chain is separated into two parts: (1) a systematic part represented by phenomenological damping (with friction constant $\bar{\eta}$), and (2) a rapidly fluctuating part $\bar{R}(\bar{t})$ which characterizes the Brownian motion aspect of the system.

As discussed in Sec. I, the periodic potential is chosen to be continuous and piecewise quadratic having the form

$$\bar{U}(\bar{x}) = \begin{cases} \frac{1}{2} k_2 \bar{x}^2, & |\bar{x}| \leq \phi \\ \frac{1}{4} k_2 \phi - [(k_2 \phi)/(b-2\phi)] (\frac{1}{2} b - |\bar{x}|)^2, & \phi \leq |\bar{x}| \leq \frac{1}{2} b. \end{cases} \quad (2.1)$$

In Fig. 1, the horizontal line separates regions of positive and negative curvature (henceforth referred to as wells and peaks, respectively). Thus, \bar{x} represents the distance from a well bottom and ϕ is the distance to change of curvature. As shown in Fig. 1, there is a portion of the chain in which there is an extra particle relative to the

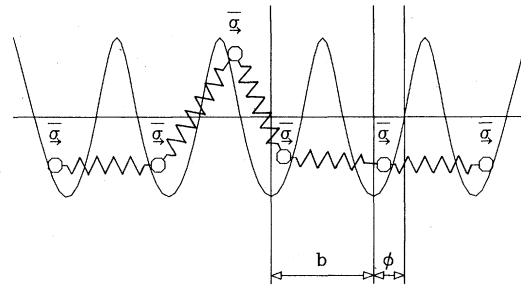


FIG. 1. Modified Frenkel-Kontorova model. Potential is piecewise quadratic with periodicity b . ϕ is the distance to change of curvature. $\bar{\sigma}$ is the applied stress on each atom. Atoms subject to potential with negative curvature (above the horizontal line) are referred to as weak-bond atoms; those below the line are referred to as strong-bond atoms.

number of available potential wells. In the configuration shown, the extra atom appears on a potential peak. What is of interest is the dynamics of this configuration.

Thus far, the model has been described in rather general terms. At this point we make the connection to dislocations both because of previous development and for the physical insight that may be obtained from such a viewpoint. However, it should be emphasized that what follows is not dependent upon the dislocation picture and can be applied as well to the other physical situations mentioned in the Introduction.

In this context then, we are describing a modified Frenkel-Kontorova model of an edge dislocation. The linear chain represents the slip-plane atoms, the periodic potential depicts the effect of the remaining atoms in the crystal (in the original Frenkel-Kontorova model this substrate potential was sinusoidal), and the atom on the substrate potential peak in Fig. 1 indicates the dislocation position. The external field $\bar{\sigma}$ is representative of an applied shear stress. Thermal effects in the crystal (i.e., the thermal vibrations of the crystal atoms surrounding the shear plane) are modeled by the heat bath whose interaction with the slip-plane atoms is described by the Langevin approach. Our interest lies in the propagation of the dislocation down the length of the chain under varying conditions of stress, viscosity, and temperature.

From this model we obtain the following equations of motion for the i th atom:

$$m \frac{d^2 \bar{x}_i}{dt^2} = -\bar{\eta} \frac{d\bar{x}_i}{dt} + k_1 (\bar{x}_{i+1} - 2\bar{x}_i + \bar{x}_{i-1}) + \bar{F}(\bar{x}_i) + \bar{\sigma} + \bar{R}_i(\bar{t}), \quad \bar{F}(\bar{x}_i) = -d\bar{U}(\bar{x}_i)/d\bar{x}_i. \quad (2.2)$$

As usual, the superposed dot will be used to denote differentiation with respect to time, and the rapidly fluctuating force term $\bar{R}_i(\bar{t})$ is assumed to be distributed in a Gaussian fashion with mean and covariance

$$\langle \bar{R}_i(\bar{t}) \rangle = 0, \quad \langle \bar{R}_i(\bar{t}) \bar{R}_i(\bar{t}') \rangle = 2\bar{\eta}k_B\bar{T}\delta(\bar{t} - \bar{t}'), \quad (2.3)$$

with k_B denoting Boltzmann's constant. Employing the following dimensionless variables:

$$\begin{aligned} x_i &= \bar{x}_i/b, \quad \sigma = \bar{\sigma}/k_2b, \quad \gamma = \phi/b, \\ P &= k_2/k_1, \quad Q = 2\gamma P/(1 - 2\gamma), \quad t = (k_1/m)^{1/2}\bar{t}, \end{aligned} \quad (2.4)$$

$$T = k_B\bar{T}/(k_1b^2), \quad \bar{\eta} = (k_1/m)^{1/2}\bar{\eta},$$

the defining equation of the model takes the form

$$\begin{aligned} \ddot{x}_i &= -\eta\dot{x}_i + x_{i+1} - 2x_i + x_{i-1} + F(x_i) + P\sigma + R_i(t), \\ F(x_i) &= \begin{cases} -P\xi_i, & |\xi_i| \leq \gamma \\ \mp Q(\frac{1}{2} \mp \xi_i), & \gamma < |\xi_i| \leq \frac{1}{2} \end{cases} \end{aligned} \quad (2.5)$$

where ξ_i is the position of the i th atom relative to the nearest well with the sign chosen for ξ_i positive or negative, respectively:

$$\begin{aligned} \langle R_i(t) \rangle &= 0, \\ \langle R_i(t) R_i(t') \rangle &= 2\eta T \delta(t - t'). \end{aligned}$$

III. LOCAL-MODE APPROXIMATION: $T = 0$

For $T = 0$, the fluctuating term $R_i(t)$ in Eq. (2.5) is absent and we have a purely deterministic set of equations to describe the chain. Except for the presence of the viscous force, this is the same situation as encountered in I and II. Following the nomenclature of I, we shall refer to atoms in wells as strong-bond atoms and to those on peaks as weak-bond atoms. The number of weak bonds for a dislocation in static equilibrium depends on the parameters P and γ . As shown in I, for a given set of P and γ there exist two equilibrium configurations for the dislocation. One, with N_w weak bonds, is a stable equilibrium configuration. The second, with $N_w + 1$ weak bonds, is an unstable equilibrium configuration. This situation holds as long as the applied stress σ is less than a critical stress σ_p (termed the Peierls stress in dislocation theory); for $\sigma = \sigma_p$ no stable equilibrium solution exists. Calculations for the positions of the atoms in the two equilibrium configurations are presented in I and, being static calculations, they are unaffected by the inclusion of viscosity.

In this paper we confine attention to parameters P and γ such that²⁷ $N_w = 1$. As described in detail in II, the dislocation propagates along the chain by undergoing a succession of transitions from stable (S) to unstable (U) states (Fig. 2), where the

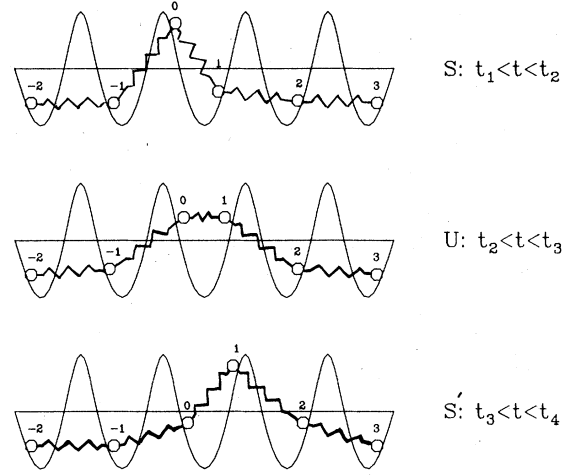


FIG. 2. Sequence of atom states during dislocation motion. Stable states, S and S' , are ones in which there is one weak-bond atom. Unstable state U has two weak-bond atoms.

terms stable and unstable refer only to the number of weak bonds present in each period. Following II, we describe the motion of the atoms during the time intervals when the chain is in an $S(U)$ state, in terms of their displacements from the stress-free stable (unstable) equilibrium positions calculated in I. This enables us to write the equations of motion in the following form:

$$\ddot{q}_i^S + \eta\dot{q}_i^S + \sum_j S_{ij}q_j^S = P\sigma, \quad t_1 < t < t_2 \quad (3.1a)$$

$$\ddot{q}_i^U + \eta\dot{q}_i^U + \sum_j U_{ij}q_j^U = P\sigma, \quad t_2 < t < t_3 \quad (3.1b)$$

where $q_i^{S,U}$ is the displacement from the stable (unstable) stress-free equilibrium configurations appropriate to the time period. S_{ij} and U_{ij} are the potential-energy matrices of the system when it is in a stable or unstable state, respectively. When the weak-bond atoms correspond to $i = 0$ in the stable state and to $i = 0, 1$ in the unstable state, they take the form

$$\begin{aligned} S_{ij} &= 2 + P, \quad |j| > 0, \quad U_{ij} = 2 + P, \quad |j| > 1 \\ S_{00} &= 2 - Q = U_{00} = U_{11}, \\ S_{j,j+1} &= S_{j+1,j} = U_{j,j+1} = U_{j+1,j} = -1, \quad |j| > 0 \\ S_{ij} &= U_{ij} = 0, \quad |i - j| > 1. \end{aligned} \quad (3.2)$$

We let λ_α^S , $\alpha = 0, 1, 2, \dots$, equal the eigenvalues of the matrix S_{ij} and let α_α^S be the associated unit eigenvectors. The eigenvalues are ordered in increasing magnitude and α_α^S is the displacement of the j th atom in the α th mode. Similarly, we let λ_α^U and α_α^U be associated with U_{ij} . Introducing the normal coordinates

$$\dot{Q}_\alpha^S = \sum_j a_{\alpha j}^S \dot{q}_j^S, \quad q_j^S = \sum_\alpha a_{\alpha j}^S Q_\alpha^S \quad (3.3a)$$

$$\dot{Q}_\alpha^U = \sum_j a_{\alpha j}^U \dot{q}_j^U, \quad q_j^U = \sum_\alpha a_{\alpha j}^U Q_\alpha^U \quad (3.3b)$$

we can write Eqs. (3.1a) and (3.1b) as

$$\ddot{Q}_\alpha^S + \eta \dot{Q}_\alpha^S + \lambda_\alpha^S Q_\alpha^S = P \sigma \sum_i a_{\alpha i}^S, \quad t_1 < t < t_2 \quad (3.4a)$$

$$\ddot{Q}_\alpha^U + \eta \dot{Q}_\alpha^U + \lambda_\alpha^U Q_\alpha^U = P \sigma \sum_i a_{\alpha i}^U, \quad t_2 < t < t_3. \quad (3.4b)$$

As noted in II, for a wide range of parameter values, the eigenvectors a_{0j}^S and a_{0j}^U correspond to localized modes, i.e., they have appreciable magnitude only in the vicinity of the dislocation. These localized modes $a_{0j}^S(a_{0j}^U)$ correspond to the minimum eigenvalue $\lambda_0^S > 0$ ($\lambda_0^U < 0$) in the $S(U)$ state. As discussed in greater detail in II, this allows us to make the approximation in the vicinity of the dislocation (i.e., for small $|j|$) that

$$q_j^S = a_{0j}^S Q_0^S, \quad t_1 < t < t_2 \quad (3.5a)$$

$$q_j^U = a_{0j}^U Q_0^U, \quad t_2 < t < t_3. \quad (3.5b)$$

With the use of these relations, it is possible to develop (as described in II) an approximate formulation for the dynamics of the dislocation solely in terms of the localized modes. We refer to this approximation as the local-mode approximation (LMA) and it is one of the purposes of this paper to explore its accuracy in the presence of viscosity and thermal motion.

In II, the total traverse of each localized normal coordinate is shown to be

$$d_S = Q_0^S(t_2) - Q_0^S(t_1) = 2q_1^S(t_2)/a_{01}^S, \quad (3.6a)$$

$$d_U = Q_0^U(t_3) - Q_0^U(t_2) = -2q_1^U(t_2)/a_{01}^U. \quad (3.6b)$$

Also, since $q_j^S(t)$ and $q_j^U(t)$ differ only in their fixed references, $q_j^S(t) = q_j^U(t)$ and therefore

$$\begin{aligned} \dot{Q}_0^U(t_2) &= \sum_j a_{0j}^U \dot{q}_j^U(t_2) = \sum_j a_{0j}^U \dot{q}_j^S(t_2) \\ &\simeq \sum_j a_{0j}^U a_{0j}^S \dot{Q}_0^S(t_2) = B^{1/2} \dot{Q}_0^S(t_2), \end{aligned} \quad (3.7)$$

where

$$0 < B^{1/2} = \sum_j a_{0j}^U a_{0j}^S < 1. \quad (3.8)$$

Similar equations are found for the next transition time t_3 and for succeeding transition times.

This leads to the interpretation, first shown in II, that we may regard the local normal coordinates as describing the motion of a series of alternately suspended (stable) and inverted (unstable) pendulums that are subject to a constant force and which transfer energy to their successors

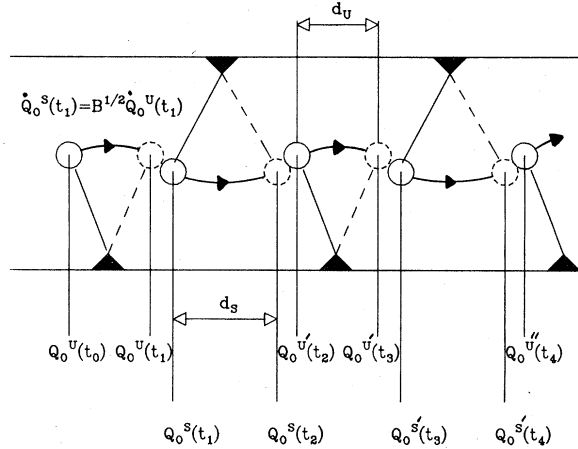


FIG. 3. Pendulum interpretation of the motion of the localized modes through stable (S) and unstable (U) states. The motion of each successive pendulum is initiated by an inelastic collision with its predecessor, with the momentum transfer reduced by $B^{1/2}$ [Eq. (3.7)].

through inelastic (since $B < 1$) collisions. In the present treatment the pendulums are, in addition, immersed in a viscous fluid (Fig. 3). This pendulum analogy should not be confused with the mechanical analogy frequently used for the sine-Gordon chain in which an angle variable is used for the displacement of each particle and the chain then corresponds to a system of torsion-coupled pendulums. Here the pendulums correspond to the local normal coordinates and are coupled to each other only through inelastic impacts at transition times.

A. Dynamic Peierls stress

As shown in I and II, there are two critical stresses associated with the model. One previously mentioned is the Peierls stress (σ_P). In addition to the earlier definition, it may also be regarded as the stress required to move the dislocation quasistatically from one stable equilibrium position to an adjacent one. Clearly, the value of this critical stress is unaffected by the presence of viscous damping. However, as pointed out in II, once the dislocation has crossed one potential barrier, continued motion is possible at lower stress levels. The minimum stress necessary to maintain dislocation motion is termed the dynamic Peierls stress (σ_{PD}) and is calculated in II for the case of $\eta = 0$. For nonzero η , the value of σ_{PD} increases as there is now another mechanism for energy loss in addition to the inelastic transfer of energy during transitions between S and U states.

To compute the effect of viscosity upon σ_{PD} on the basis of the local-mode approximation we

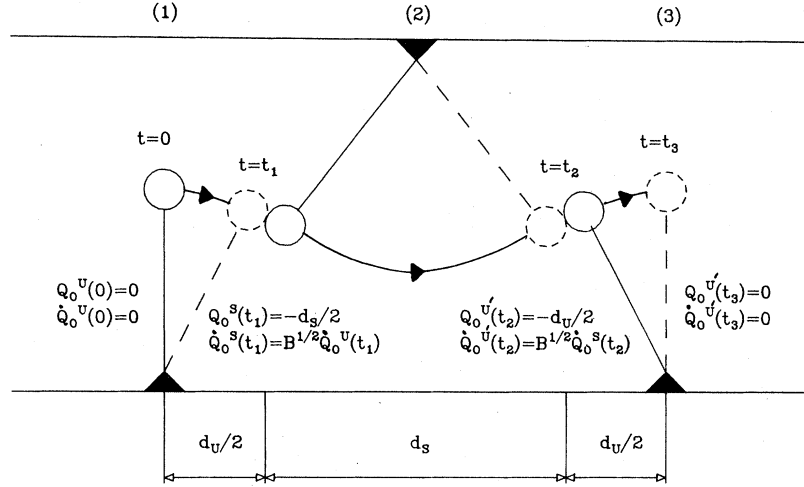


FIG. 4. Employment of the pendulum analogy to calculate $\sigma_{PD}(\eta)$. This is the stress that will move the pendulums through the sequence (1)-(2)-(3) and provides a local-mode approximation for the minimum stress required to sustain dislocation motion once motion has been initiated.

proceed as follows. Since σ_{PD} is the stress just sufficient to continue dislocation motion, we see from the pendulum analogy that the problem of calculating σ_{PD} is equivalent to determining the stress necessary to produce the following process (Fig. 4). We start the first unstable pendulum in its upright ($Q_0^U = 0$) position at $t = 0$ with zero velocity and let it strike the stable pendulum which then hits the next unstable one. σ_{PD} is then the stress such that the second unstable pendulum arrives at its upright position with zero velocity.

The solutions to Eqs. (3.4a) and (3.4b) during each time period are (omitting superscripts S and U),

$$Q_0(t) = \frac{1}{(\mu_2 - \mu_1)} [(x_0 \mu_2 - u_0) e^{\mu_1 t} - (x_0 \mu_1 - u_0) e^{\mu_2 t}] + \frac{A}{\mu_1 \mu_2 (\mu_1 - \mu_2)} (\mu_1 - \mu_2 + \mu_2 e^{\mu_1 t} - \mu_1 e^{\mu_2 t}), \quad (3.9a)$$

$$\dot{Q}_0(t) = \frac{1}{(\mu_1 - \mu_2)} [\mu_1 (x_0 \mu_2 - u_0) e^{\mu_1 t} - \mu_2 (x_0 \mu_1 - u_0) e^{\mu_2 t}] + \frac{A}{(\mu_1 - \mu_2)} (e^{\mu_1 t} - e^{\mu_2 t}), \quad (3.9b)$$

where, during a period corresponding to a stable state,

$$\mu_{1,2} = -\frac{1}{2} \eta \pm (\frac{1}{4} \eta^2 - \omega_s^2)^{1/2}, \quad (3.10a)$$

$$\omega_s^2 = \lambda_0^S, \quad A = P \sigma a_s = P \sigma \sum_i a_{oi}^S,$$

and during a period corresponding to an unstable state,

$$\mu_{1,2} = -\frac{1}{2} \eta \pm (\frac{1}{4} \eta^2 + \omega_U^2)^{1/2}, \quad (3.10b)$$

$$\omega_U^2 = -\lambda_0^U, \quad A = P \sigma a_U = P \sigma \sum_i a_{oi}^U.$$

$x_0 = Q_0(0)$ and $u_0 = \dot{Q}_0(0)$ are the starting positions and velocities for Q_0^S, U for each time interval. Since $Q_0^U(0)$ and $\dot{Q}_0^U(0)$ are known, Eq. (3.9a) provides $Q_0^U(t)$. Then t_1 is determined so that $Q_0^U(t_1) = \frac{1}{2} d_U$. This enables us to obtain $\dot{Q}_0^S(t_1) = B^{1/2} \dot{Q}_0^U(t_1)$ and calculate $Q_0^S(t)$ for $t > t_1$; t_2 is then determined and so forth. The equations for t_1 and t_2 are transcendental and are solved numerically using a bisection method. As a further simplification, we do not need to calculate t_3 since we know that the coefficients of the growing exponential must be zero in order for $Q_0^U(t_3)$ to arrive at zero, where U' denotes the unstable state which starts at $t = t_2$. Thus we have

$$P \sigma a_U / \mu_1^{U'} = x_0^{U'} \mu_2^{U'} - u_0^{U'} \quad (3.11)$$

as a criterion for $\sigma_{PD}(\eta)$.

The computation procedure used was to begin with a particular stress, calculate t_1 and t_2 , and evaluate Eq. (3.11). If the difference between the left- and right-hand sides was greater than 1.0×10^{-6} , the stress was changed accordingly and t_1 and t_2 recalculated until the zero criterion was met to the desired accuracy.

The results of this calculation may be seen in Fig. 5. As a check, the value obtained analytically in II for $\sigma_{PD}(\eta = 0)$ is 3.06×10^{-4} for $P = 0.5$ and $\gamma = 0.3$, and the above procedure yields the same result. It is also seen from this figure that the value of σ_{PD} computed on the basis of the LMA approaches a constant value for large η . The limit-

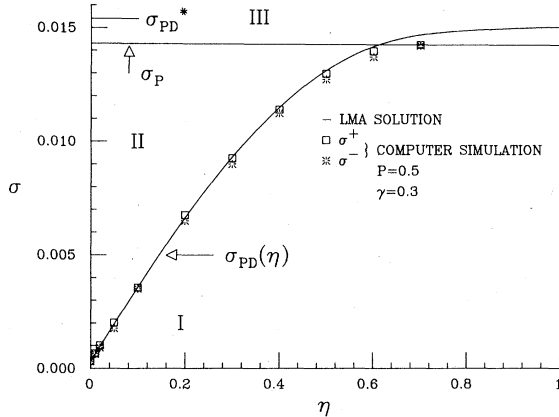


FIG. 5. Characterization of dislocation motion in terms of the stress and the viscosity for $T=0$ K. Region I has only "locked" solutions, region II has only "running" solutions. Region II has both running and locked solutions, depending on whether the initial chain configuration was stable or unstable. Regions II and III are separated by the Peierls stress σ_P , and regions I and II are separated by the dynamic Peierls stress σ_{PD} , whose value depends on η . σ_{PD}^* is the limiting value of σ_{PD} for large η as computed on the basis of the local-mode approximation. The computer simulation employed a time step $\delta t=0.07$, with the propagation or nonpropagation of the dislocation being determined by graphic display of atomic trajectories.

ing value may be computed analytically by neglecting the inertia term in the equation of motion for Q_0^U , Eq. (3.4b), so that it takes the form

$$\eta \dot{Q}_0^U(t) - \omega_D^2 Q_0^U(t) = P\sigma a_V. \quad (3.12)$$

The solution to Eq. (3.12) with initial condition $Q_0^U(0) = -\frac{1}{2}d_V$ is

$$Q_0^U(t) = e^{(\omega_D^2/\eta)t} \left(-\frac{1}{2}d_V + \frac{P\sigma a_V}{\omega_D^2} \right) - \frac{P\sigma a_V}{\omega_D^2},$$

and it is seen that continued motion is not possible if $\sigma > \sigma_{PD}^*$ where

$$\sigma_{PD}^* = \omega_D^2 d_V / (2P\sigma a_V) = 0.0154$$

for the given parameter values. σ_{PD}^* is, therefore, the limiting value of σ_{PD} for large η as computed on the basis of the LMA. On the other hand, it is to be expected that for large η , σ_{PD} should approach σ_P , for the latter is the stress required to move the dislocation quasistatically along the chain. Shown also in Fig. 5 is the exact value of σ_P computed on the basis of the theory of I. The slight discrepancy between σ_{PD}^* and σ_P is a measure of the accuracy of the local-mode approximation. The accuracy of the approximation for σ_{PD} for small η will be discussed in Sec. V on the basis of computer simulation calculations.

We see from Fig. 5 that there are three regions

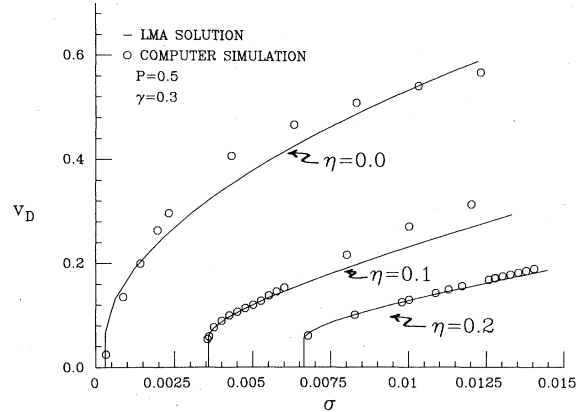


FIG. 6. Stress dependence of steady-state dislocation velocity for $T=0$ K; comparison of local-mode analysis and numerical calculations for three values of η . For the numerical calculations, a time step $\delta t=0.07$ was employed, an induction period of $t=30$ was allowed for steady-state conditions to develop, and velocities were obtained by Eq. (5.2) with a period of $t=50$. If one considers a simple harmonic oscillator in a well of curvature λ_0^S , then for these units and parameter values critical damping is given by $\eta=0.75$.

separated by σ_{PD} and σ_P that characterize the dislocation motion: In region I there is no dislocation motion. This is termed a "locked" solution by Vollmer and Risken²⁸ in their treatment of a single particle in a periodic potential. In region III, dislocation motion occurs (termed "running" solution) and in II, locked and running solutions coexist depending on whether the initial conditions correspond to the dislocation starting from rest in a stable or unstable equilibrium configuration.

B. Steady-state dislocation velocities

The localized-mode approximation can also be used to calculate the steady-state dislocation velocities in the regions in which they exist. In this case, for $\sigma > \sigma_{PD}(\eta)$, the motion of a succession of pendulums is calculated by evaluating t_1 , t_2 , and t_3 (Fig. 4) as in determining σ_{PD} , but with the stress maintained constant and with the motion allowed to continue to the next pendulum. This computation is continued until steady-state conditions are reached, at which point the dislocation velocity is given by $(t_1 + t_2 + t_3)^{-1}$. The results may be seen in Fig. 6. We defer the discussion of these results to Sec. V, where they will be compared with computer simulation calculations.

IV. COMPUTER SIMULATION

In order to evaluate the accuracy of the local-mode approximation, we need for comparison a solution that takes into account all of the normal

modes. This is obtained by the direct numerical solution of the equations of motion, Eqs. (2.5). For $T=0$, a finite-difference method was used to compute $\sigma_{PD}(\eta)$ and the dislocation velocity as a function of applied stress, and for $T>0$ a modified Runge-Kutta method was adopted.

A. $T=0$: Finite-difference method

In this approach, a finite-difference approximation was used to solve Eqs. (2.5) in which, for a given time step δt , the acceleration and velocity of each atom at time $t=n\delta t$ are given by

$$\ddot{x}_i^n = (x_i^{n+1} - 2x_i^n + x_i^{n-1})/(\delta t)^2, \quad (4.1a)$$

$$\dot{x}_i^n = (x_i^{n+1} - x_i^n)/(\delta t), \quad (4.1b)$$

where $x_i^n = x_i(n\delta t)$.

End conditions were treated as by Weiner *et al.*,²² where the motion of the "end-plus-one" atoms was determined by a convolution integral involving the motion of the "end" atoms and the propagation of a small displacement in a semi-infinite chain. This procedure is made possible by the localized nature of the dislocation, so that the equations of motion for the atoms in the outlying areas of the chain are linear. Therefore it is only necessary to simulate explicitly a finite chain, atoms indexed $i=1$ to N , and to use the convolution theorem to express the motion of atoms $i=0$ and $i=N+1$ in terms of atoms $i=1$ and N , respectively. This procedure is implemented as follows. First consider a semi-infinite chain with defining equations

$$\ddot{v}_k = v_{k+1} - (2+P)v_k + v_{k-1} - \eta \dot{v}_k, \quad k \geq 0 \quad (4.2b)$$

$$v_k(0) = \dot{v}_k(0) = 0, \quad (4.2b)$$

$$v_0(t) = 1. \quad (4.2c)$$

Equation (4.2a) describes the displacements of the atoms of a chain in which the atoms remain in the harmonic region of the substrate potential. By use of the convolution theorem it then follows that

$$u_{N+1}(t) = \int_0^t u_N(t-\tau) \dot{v}_1(\tau) d\tau, \quad (4.3a)$$

$$u_0(t) = \int_0^t u_1(t-\tau) \dot{v}_1(\tau) d\tau, \quad (4.3b)$$

where $u_i(t)$ is the displacement of the i th atom from the minimum of its substrate potential well. Equations (4.3) were used to provide $x_0(t)$ and $x_{N+1}(t)$ for Eqs. (2.5) and thereby to simulate an infinite chain.

Equations (4.2) were solved using the finite-difference method and values for $v_1^n = v_1(n\delta t)$ were stored. The integrals were evaluated by the approximation

$$u_{N+1}^n = u_{N+1}(n\delta t) = \sum_{m=1}^n u_N^{n-m} (v_1^m - v_1^{m-1}). \quad (4.4)$$

This sum can be truncated for sufficiently large m , $m > m_L$ as $v_1^{mL} - v_1^{mL-1} \sim 0$. A similar approximation was used for Eq. (4.3b).

B. $T>0$: Modified Runge-Kutta method

In this approach we used a Runge-Kutta technique adapted to stochastic differential equations as developed by Helfand.²⁹ The procedure (presented first for a single equation for simplicity) is as follows. To solve

$$dy/dt = f(y) + R(t), \quad (4.5a)$$

$$\langle R(t) \rangle = 0, \quad \langle R(t)R(t') \rangle = \xi \delta(t-t'), \quad (4.5b)$$

Helfand derives the algorithm

$$g_1 = f(y_0 + \delta t^{1/2} \xi^{1/2} \lambda_1 z), \quad (4.6a)$$

$$g_2 = f(y_0 + \delta t \beta g_1 + \delta t^{1/2} \xi^{1/2} \lambda_2 z), \quad (4.6b)$$

$$y = y_0 + \delta t (A_1 g_1 + A_2 g_2) + \delta t^{1/2} \xi^{1/2} \lambda_0 z. \quad (4.6c)$$

z is a Gaussian random variable with mean zero and variance unity generated at each time step δt . The constants are

$$A_1 = A_2 = \frac{1}{2}, \quad \beta = 1, \quad (4.7)$$

$$\lambda_0 = 1, \quad \lambda_1 = 0, \quad \lambda_2 = 1.$$

The generalization to a system of $2N$ equations (where N = the number of atoms) is done by considering y , A , and f as vectors of length $2N$ with elements

$$y_i = \begin{cases} \dot{x}_i, & i \text{ odd} \\ x_i, & i \text{ even} \end{cases} \quad (4.8a)$$

$$R_i = \begin{cases} R_i(0), & i \text{ odd} \\ 0, & i \text{ even} \end{cases} \quad (4.8b)$$

$$f_i = \begin{cases} x_{i+1} - 2x_i + x_{i-1} - \eta \dot{x}_i + P\sigma + F(x_i), & i \text{ odd} \\ \dot{x}_i, & i \text{ even} \end{cases}$$

$$\xi = 2\eta T.$$

In this form, y , R , and f when substituted into Eqs. (4.5) yield Eqs. (2.5). End conditions were treated as before, where, within a time step δt , the end-plus-one atoms x_0 and x_{N+1} were kept fixed for calculating the end components of g_1 and g_2 , with new values for x_0 and x_{N+1} calculated for the next time step. This procedure does not precisely mimic an infinite chain for the case $T>0$ since random force effects are not included for the two semi-infinite linear chains treated by the convolution integral. However, this effect should be small for sufficiently large N and check calcula-

tions did not reveal any significant size effect.

As a check on Helfand's method, trajectories and time-averaged velocities were calculated for single particles in a harmonic well. For suitable time steps and averaging over a sufficient number of replicas, the agreement with the exact solution was good. Results of the computer simulation calculations both for $T=0$ and $T>0$ are presented in Sec. V.

V. NUMERICAL CALCULATIONS: $T=0$

A. Dynamic Peierls stress

Using the finite-difference method described in Sec. IV, we determined $\sigma_{PD}(\eta)$ in the following manner: For a given η , a stress σ was chosen and the configuration corresponding to unstable equilibrium under the applied stress σ was used for the initial atom positions; initial atom velocities were zero. The motion of the atoms was then allowed to develop as dictated by Eqs. (4.1) and (2.5). If the dislocation moved over one or more wells, the stress was considered above σ_{PD} and designated σ^+ . Similarly, if the dislocation remained in its initial well, the stress was below σ_{PD} and designated σ^- . This process was continued until a narrow bracketing was achieved with the result that $\sigma^- < \sigma_{PD} < \sigma^+$. The values of σ^+ and σ^- are presented in Fig. 5. The agreement with the values of σ_{PD} obtained by the localized-mode approximation was very good.

B. Dislocation velocity

To determine dislocation velocities for a given η , a stress $\sigma > \sigma_{PD}(\eta)$ was chosen. Initial atom positions were those of the unstable equilibrium configuration for that stress, and initial velocities were zero. The simulation was allowed to proceed until a steady-state condition for the dislocation motion was reached. As a measure of dislocation velocity, we used

$$v_D(t) = \sum_{i=1}^N \dot{x}_i(t). \quad (5.1)$$

Equation (5.1) may be justified on the basis of arguments as in Sec. IV of I. To remove fluctuations, we used a time-averaged velocity given by

$$\langle v_D(t) \rangle = \frac{1}{t} \int_0^t \sum_i \dot{x}_i(t) dt = \frac{1}{t} \sum_i [x_i(t) - x_i(0)]. \quad (5.2)$$

A representative plot of $\langle v_D(t) \rangle$ is given in Fig. 7 for $\sigma = 0.0080$.

The above procedure was repeated for various values of σ and for values of $\eta = 0.0, 0.1, \text{ and } 0.2$. Plots of the steady-state dislocation velocities

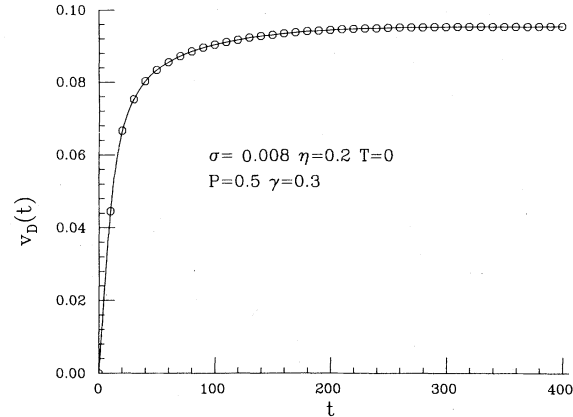


FIG. 7. Example of the time development of the dislocation velocity at $T=0$ as obtained by computer simulations. The calculation used the Runge-Kutta method, Eqs. (4.6)–(4.8), with T set equal to zero and a time step of $\delta t = 0.05$. Velocities were obtained by Eq. (5.2).

(v_D) as a function of stress are shown in Fig. 6. We note that for all values of η the agreement with the local-mode approximation is fairly good and the agreement becomes excellent for $\eta = 0.2$. We also note that there is a departure at higher stress levels from the LMA for all three values of η (though the departure is difficult to see for $\eta = 0.2$). We believe that the departure is due to the loss of dominance of the localized mode due to the activation of higher modes. Increased viscosity seems to cause damping of these higher modes and restores the localized mode to being the controlling factor in the dislocation velocity.

C. Dislocation velocity in original Frenkel-Kontorova model

A natural question which arises is the degree to which the behavior of the modified Frenkel-Kontorova model, for an appropriate choice of parameters, approximates the behavior of the original Frenkel-Kontorova model. For this purpose, computer simulation calculations were performed to determine the stress dependence of dislocation velocity in the original model, that is, one identical to the modified model except that the substrate potential is given by

$$V(x) = (P\gamma/2\pi)(1 - \cos 2\pi x)$$

in place of Eq. (2.1). The method of calculation, except for the definition of the potential, was identical to that employed for the modified model. The results are shown in Fig. 8 where they are compared with the local-mode approximation to the modified model with parameter values $P = 0.75$ and $\gamma = 0.25$, and it is seen that the agreement is very good. The choice of parameter values was

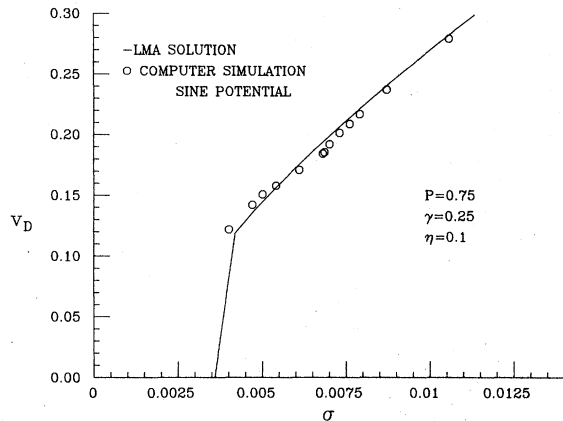


FIG. 8. Results of local-mode approximation to original Frenkel-Kontorova model or sine-Gordon chain as compared with computer simulation results for dislocation or kink velocity as a function of applied stress.

dictated by the following considerations. It is clear that $\gamma = 0.25$ provides the best fit, as far as the applied force is concerned, of the piecewise quadratic function of Eq. (2.1) to the sinusoidal potential (Fig. 9). The value of $P = 0.75$ was then chosen to lie in the range of parameters which leads to a single local mode in both stable and unstable equilibrium configurations.

VI. NUMERICAL CALCULATION: $T > 0$

For $T > 0$, the modified Runge-Kutta method described in Sec. IV was used. The temperature levels studied were chosen in relation to the energy barrier (at zero stress) between a stable and unstable configuration. In I this energy barrier was calculated to be

$$\bar{E}_B(\sigma) = \frac{(\sigma_P - \sigma)^2}{4\sigma_P} k_2 b^2 = \frac{(\sigma_P - \sigma)^2}{4\sigma_P} P k_1 b^2. \quad (6.1)$$

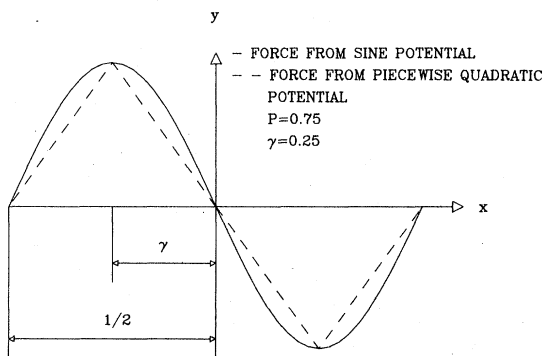


FIG. 9. Comparison of force derived from sine potential and that derived from the piecewise quadratic potential.

Introducing the dimensionless energy barrier E_B ,

$$E_B(\sigma) = \bar{E}_B(\sigma)/(k_1 b^2),$$

and for the parameter values used in the calculations ($P = 0.5$ and $\gamma = 0.3$), $E_B(0) = 0.00178$.

In determining the initial conditions with which to begin the simulation, different considerations apply in the three stress regions. (a) For $\sigma < \sigma_{PD}$ it is clear from the preceding discussion that the occasional surmounting of potential barriers with the aid of thermal activation is necessary in order for the dislocation to achieve some average steady-state velocity. Thus, it is immaterial from a theoretical point of view as to whether or not the simulation is begun in the stable or unstable configuration. However, from a practical point of view, one sees that a simulation begun in the unstable configuration, because of its dynamic instability at the crest of a potential barrier, has a strong probability of either being greatly assisted or greatly hindered by the thermal motion in its early time development and therefore requires a longer time to come to a steady-state condition. For this reason, the simulation was begun in the stable configuration for $\sigma < \sigma_{PD}$. (b) For $\sigma_{PD} < \sigma < \sigma_P$, continued dislocation motion is possible without thermal activation if the dislocation begins from an unstable configuration, although it may get stopped by adverse thermal motion and require thermal activation for restarting. Thus there is again the choice of starting from either a stable or unstable equilibrium configuration. Although the two should converge ultimately to the same steady-state value, the approach appeared more rapid for the cases in which the dislocation began from a stable equilibrium configuration, and this initial condition was used in this stress interval as well. (c) For $\sigma > \sigma_P$ the simulation must be started with $\sigma < \sigma_P$ and slowly increased to the desired value since there is no equilibrium configuration for $\sigma > \sigma_P$. Again, the initial configuration at the starting stress is chosen as stable. All atomic velocities are taken to be zero at the start of the computation.

Dislocation velocities were calculated as in Sec. V. However, it was found necessary to average over an ensemble of replicas of a chain. The numerical computations for each replica were begun with the same initial conditions but with a different seed for the random-number generator. The need for averaging is due to the fact, as previously noted, that thermal effects can halt dislocation motion (or even reverse it temporarily) and thus it must be thermally activated to begin motion again. These effects can be seen in Figs. 10 and 11 where for a single replica of the chain we have plotted atomic trajectories and the time

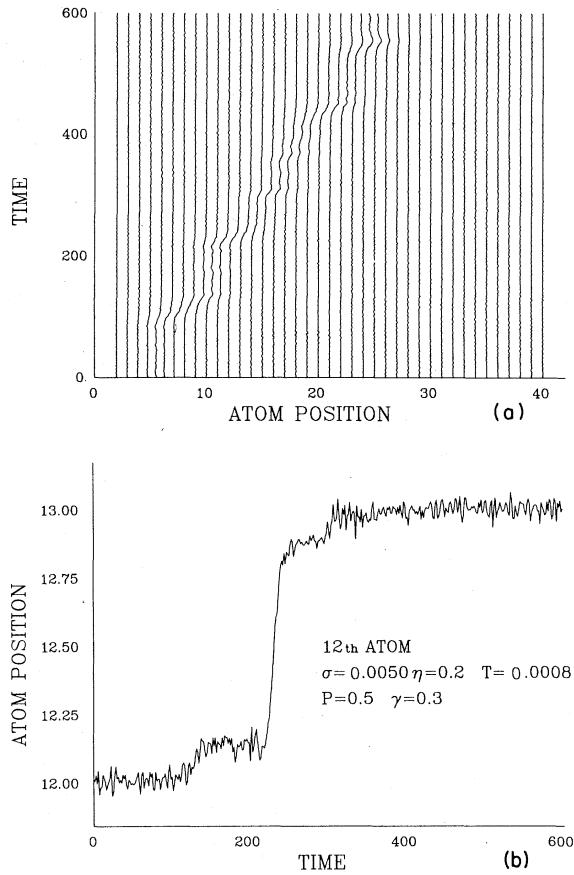


FIG. 10. (a) Atomic trajectories for a single replica of the chain for $T = 0.0008$, $\eta = 0.2$, and $\sigma = 0.005$. Note that $\sigma < \sigma_{PD}$ for this case. The chain has 40 atoms with the dislocation initially in the sixth well. (b) Enlarged trajectory of the 12th atom of the chain shown in (a).

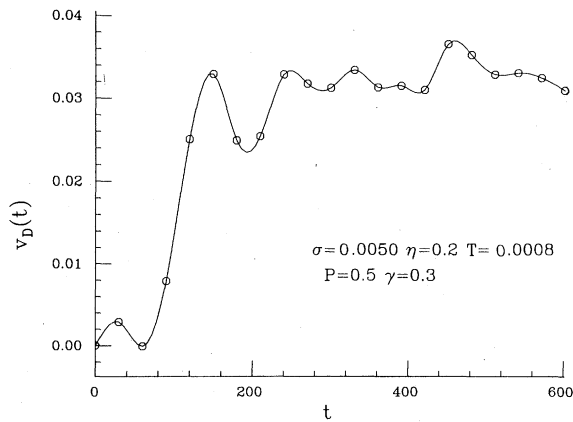


FIG. 11. Time development of dislocation velocity for the single replica of the chain shown in Fig. 10(a). The computer simulation used the Runge-Kutta method, Eqs. (4.6)–(4.8), and employed a time step of $\delta t = 0.15$. Velocities were calculated as in Eq. (5.2).

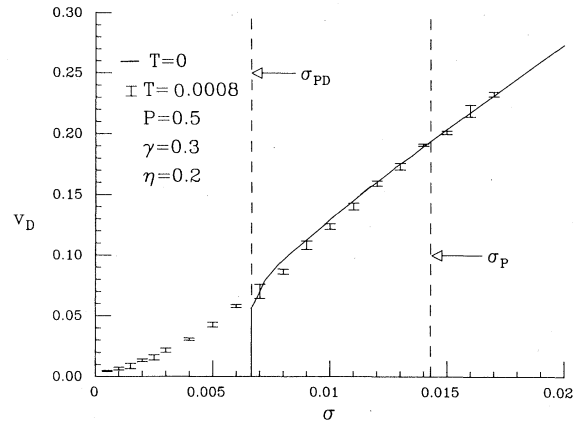


FIG. 12. Stress dependence of dislocation velocity for $T = 0.0008$ and $\eta = 0.2$. The computer simulation used a time step of $\delta t = 0.15$. Each simulation run employed between 10 and 100 replicas with their velocities calculated by Eq. (5.2). These velocities were then averaged over the replicas to produce a mean velocity for that simulation run. For each stress, several runs (at least two) were performed. The resulting mean velocities for the runs for a particular stress were weighted in proportion to the number of replicas for that run, and then averages and standard deviations calculated. The error bars indicate these standard deviations.

development of the velocity. This effect is most predominant at low stresses where thermal motion is essentially the sole activator of dislocation motion and hence the largest number of replicas were used here.

In Figs. 12 and 13 we have plotted dislocation

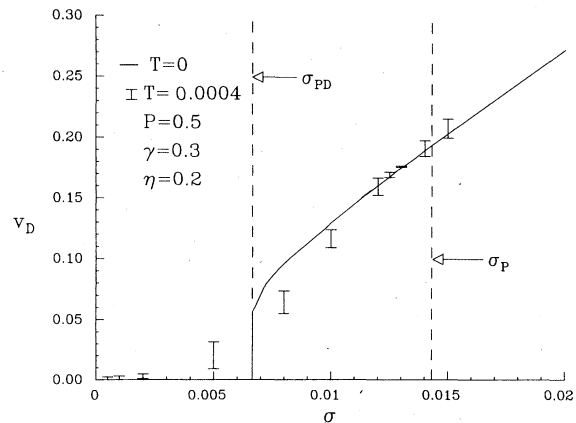


FIG. 13. Stress dependence of dislocation velocity for $T = 0.0004$ and $\eta = 0.2$. In this case in general, only a single simulation run was made at each stress level, with between 10 and 50 replicas for each run. Error bars denote the standard deviation for the ensemble of replicas. To examine the effect of enhanced velocity at elevated temperature at $\sigma = 0.0125$ and 0.0130 , additional computer simulation runs were made and error bars calculated as described in the caption for Fig. 12.

velocity versus stress for $\eta=0.2$, $T=0.008$, and $T=0.004$. The solid line represents the $T=0$ solution as developed by the computer simulation.

VII. CONCLUSIONS

The following conclusions can be drawn from the present work.

(1) The local-mode approximation may be used when the model parameter values are in the range for which there is a single localized mode in both stable and unstable equilibrium configurations and it provides a transition from the sine-Gordon chain, with an infinite number of degrees of freedom, to a system with a single degree of freedom.³⁰ With Brownian motion included, this approximation provides, therefore, a close analogy between the sine-Gordon chain and the model of a particle undergoing Brownian motion while subject to a periodic potential and to an external driving force. The latter model has been studied extensively in its own right as a model for the diffusion of impurity atoms in a crystal,³¹ for the study of superionic conductors, and for its intrinsic interest.^{28,32} Although the analogy is close, it is not complete since a residue of the many degrees of freedom of the sine-Gordon chain remains in the inelastic collisions of the pendulum analogy (Fig. 3) suggested by the local-mode approximation.

(2) The local-mode approximation gives accurate results³³ (Fig. 5) for the computation of $\sigma_{PD}(\eta)$, the stress required at $T=0$ K to maintain dislocation motion once it has been initiated in a medium of viscosity η .

(3) The local-mode approximation gives accurate results (Fig. 6) for the steady-state velocity achieved by a dislocation at $T=0$ K when it starts under a constant applied stress from an unstable equilibrium position. The accuracy is particularly good at low stress values while at higher stress levels it appears that other modes are excited. The agreement becomes better as the viscosity is increased, apparently because the higher-frequency modes are then suppressed.

(4) Computer simulation calculations were also performed to determine steady dislocation velocities at $T=0$ K as a function of applied stress for the original Frenkel-Kontorova model or sine-Gordon chain, in which the substrate potential is sinusoidal rather than piecewise quadratic as in the modified model. The computer simulation results were compared with the local-mode approximation for the corresponding modified model and the agreement (Fig. 7) was found to be very good.

We see, therefore, that for a suitable choice of parameters, the modified Frenkel-Kontorova model provides a good approximation to the original model or, equivalently, to the sine-Gordon chain and that the local-mode approximation may be applied to either.

(5) Computer simulations of the model for $T > 0$ K were also performed (Figs. 12 and 13). For stresses below $\sigma_{PD}(\eta)$, steady dislocation motion is not possible at $T=0$ K. For $T > 0$ K, thermal activation produces an average dislocation velocity which increases with stress and temperature. For stresses above σ_{PD} , the general effect of thermal motion is to decrease the velocity from the corresponding value at $T=0$ K. This is in agreement with the usual picture of the effect of temperature upon a steadily moving dislocation, an effect usually described as due to phonon drag. However, the computer simulation results reveal (Figs. 12 and 13) that at high stress levels there is a small stress range (at $\sim\sigma=0.014$) in which thermal effects appear to increase the dislocation velocity. This may be due to the phenomenon of "thermal energy trapping," a process discussed previously by Weiner^{19,20} and Partom.³⁰ However, the observed effect in these calculations is very small and further work is necessary before unambiguous conclusions can be drawn.

As noted in the Introduction, the sine-Gordon chain is used as a model for many different physical situations. To some extent, the nature of the physical problem dictates the type of questions considered and, of course, the terminology in different fields for the localized entity (domain wall, dislocation, kink, etc.), for the particle displacement (linear or angular), and for the driving force (applied torque, stress, magnetic field) varies. Nevertheless, the underlying mathematical structure of the model is common to all applications, and techniques developed for use in one area may prove useful in others.

ACKNOWLEDGMENTS

The computations reported on here were carried out on the Brown University Division of Engineering VAX-11/780 computer. The acquisition of this computer was made possible by grants from the U.S. National Science Foundation (Grant No. ENG78-19378), the General Electric Foundation, and the Digital Equipment Corporation. Research was supported by the National Science Foundation through the Materials Research Laboratory at Brown University.

- *This paper is based on the research of D. Perchak performed in partial fulfillment of the requirements for the Ph.D. in Physics at Brown University.
- ¹J. A. Krumhansl and J. R. Schrieffer, *Phys. Rev. B* **11**, 3535 (1974).
 - ²T. Schneider and E. Stoll, *Phys. Rev. Lett.* **41**, 1429 (1978).
 - ³H. J. Mikeska, *J. Phys. C* **11**, L29 (1978).
 - ⁴J. H. Weiner, *IEEE Trans. Magn. Mag-9*, 602 (1973).
 - ⁵S. E. Trullinger, M. D. Miller, R. A. Guyer, A. R. Bishop, F. Palmer, and J. A. Krumhansl, *Phys. Rev. Lett.* **40**, 206 (1978); **40**, 1603 (E) (1978).
 - ⁶R. A. Guyer, *Phys. Rev. B* **20**, 4375 (1979).
 - ⁷A. Barone, F. Esposito, C. J. Magee, and A. J. Scott, *Revista del Nuovo Cimento* **1**, 227 (1971).
 - ⁸J. Frenkel and T. Kontorova, *J. Phys.* **1**, 137 (1939).
 - ⁹In a recent paper, R. A. Guyer and M. D. Miller [*Phys. Rev. B* **20**, 4748 (1979)] use the term Frenkel-Kontorova model as descriptive of the sine-Gordon chain at $T \neq 0$ K. The motivation for this terminology is not clear since neither the original work of Frenkel and Kontorova nor most subsequent work in the dislocation field explicitly included the effect of thermal motion of the atoms.
 - ¹⁰F. R. N. Nabarro, *Theory of Crystal Dislocations* (Oxford University Press, London, 1967).
 - ¹¹J. Kratochvil and V. Indenbom, *Czech. J. Phys.* **13**, 814 (1963).
 - ¹²J. H. Weiner and W. T. Sanders, *Phys. Rev.* **134**, A1007 (1964), hereafter referred to as I.
 - ¹³The piecewise quadratic function is taken as continuous with continuous derivatives, i.e., it is for appropriate parameters a spline approximation to the sine function. In the rhyming tradition which led from the Klein-Gordon to the sine-Gordon equation, the modified Frenkel-Kontorova model could be referred to, therefore, as the spline-Gordon chain.
 - ¹⁴Recently [S. E. Trullinger and R. M. DeLeonardis, *Phys. Rev. A* **20**, 2225 (1979)], a chain was studied in which each atom is subject to a symmetric double-well potential which is piecewise harmonic. The behavior of this chain will be the same as that of the modified Frenkel-Kontorova model with a cusped substrate potential if attention is confined in the latter to motions in which no atom moves further than one potential well. This is the case for regular motion of a dislocation or kink along the chain, and the steady motion of kinks discussed by Trullinger and DeLeonardis in the continuum (displacive) limit can be analyzed in the discrete case by use of the local-mode approximation of I (Ref. 15) or exactly by transform methods as discussed in Refs. 16, 17, 23-25. See also the recent work of J. C. Kimball, *Phys. Rev. B* **21**, 2104 (1980), which extends the work of Ref. 16 to include viscosity.
 - ¹⁵J. H. Weiner, *Phys. Rev.* **136**, A863 (1964), hereafter referred to as II.
 - ¹⁶W. Atkinson and N. Cabrera, *Phys. Rev.* **138**, A763 (1965).
 - ¹⁷V. Celli and N. Flytzanis, *J. Appl. Phys.* **41**, 4443 (1970).
 - ¹⁸S. Ishioka, *J. Phys. Soc. Jpn.* **30**, 323 (1971); **34**, 462 (1973).
 - ¹⁹J. H. Weiner, *Phys. Rev.* **139**, A442 (1965).
 - ²⁰J. H. Weiner, in *Fundamental Aspects of Dislocation Theory*, edited by J. A. Simmons, R. de Wit, and R. Bullough [Nat. Bur. Stand. (U.S.), Spec. Publ. **317**, I 1970], p. 403.
 - ²¹J. H. Weiner and M. Pear, *Philos. Mag.* **31**, 679 (1975).
 - ²²J. H. Weiner, A. Hikata, and C. Elbaum, *Phys. Rev.* **13**, 531 (1976). This model was treated statically by W. T. Sanders, *J. Appl. Phys.* **36**, 2822 (1965).
 - ²³Y. Y. Earmme and J. H. Weiner, *Phys. Rev. Lett.* **33**, 1550 (1974).
 - ²⁴Y. Y. Earmme and J. H. Weiner, *J. Appl. Phys.* **45**, 603 (1974).
 - ²⁵Y. Y. Earmme and J. H. Weiner, *J. Appl. Phys.* **48**, 3317 (1977).
 - ²⁶Superposed bars denote dimensional quantities; corresponding dimensionless quantities will have bars omitted.
 - ²⁷Conditions on the parameter values so that this is the case are presented in I. A graph showing the regions of P - γ space for various values of N_w is given in Ref. 25. The question of the effect of initial conditions and loading path upon the final steady-state dislocation velocity were discussed by Earmme and Weiner for the case $\sigma=0$ and $T=0$ K. It was found there that the final velocity depended upon the loading path when the stress did not increase monotonically. Here we confine our attention to monotonically increasing loading paths.
 - ²⁸H. D. Vollmer and H. Risken, *Z. Phys. B* **34**, 313 (1979).
 - ²⁹E. Helfand, *Bell Syst. Tech. J.* **58**, 2289 (1979).
 - ³⁰Another approach to the development of a single degree of freedom equivalent to the modified Frenkel-Kontorova model is given by Y. Partom, *J. Appl. Phys.* **50**, 4725 (1979); **50**, 4734 (1979).
 - ³¹J. H. Weiner and R. Forman, *Phys. Rev. B* **10**, 315 (1974); **10**, 325 (1974).
 - ³²P. Nozières and G. Iche, *J. Phys.* **40**, 225 (1979).
 - ³³The choice of parameters for this figure was fortuitous in that agreement between the local-mode approximation and computer simulation results was particularly good. Spot checks for other parameter values still provided good agreement, but not as good as in Fig. 5. Agreement improved with viscosity, and in all cases tested was within 10% for $\eta=0.1$.